

Convergent adaptation to dangerous prey proceeds through the same first-step mutation in the garter snake *Thamnophis sirtalis*

Michael T.J. Hague,^{1,2} Chris R. Feldman,³ Edmund D. Brodie Jr.,⁴ and Edmund D. Brodie III¹

¹Department of Biology, University of Virginia, Charlottesville, Virginia 22904

²E-mail: mh6nf@virginia.edu

³Department of Biology, University of Nevada, Reno, Nevada

⁴Department of Biology, Utah State University, Logan, Utah

Received January 17, 2017

Accepted March 24, 2017

Convergent phenotypes often result from similar underlying genetics, but recent work suggests convergence may also occur in the historical order of substitutions en route to an adaptive outcome. We characterized convergence in the mutational steps to two independent outcomes of tetrodotoxin (TTX) resistance in separate geographic lineages of the common garter snake (*Thamnophis sirtalis*) that coevolved with toxic newts. Resistance is largely conferred by amino acid changes in the skeletal muscle sodium channel (Na_v1.4) that interfere with TTX-binding. We sampled variation in Na_v1.4 throughout western North America and found clear evidence that TTX-resistant changes in both lineages began with the same isoleucine-valine mutation (I1561V) within the outer pore of Na_v1.4. Other point mutations in the pore, shown to confer much greater resistance, accumulate later in the evolutionary progression and always occur together with the initial I1561V change. A gene tree of Na_v1.4 suggests the I1561V mutations in each lineage are not identical-by-descent, but rather they arose independently. Convergence in the evolution of channel resistance is likely the result of shared biases in the two lineages of *T. sirtalis*—only a few mutational routes can confer TTX resistance while maintaining the conserved function of voltage-gated sodium channels.

KEY WORDS: Evolutionary predictability, molecular evolution, sodium channel (Na_v1.4), tetrodotoxin (TTX).

When faced with a similar evolutionary challenge, unrelated lineages often arrive at convergent phenotypic solutions. Accumulating evidence now illustrates that many examples of phenotypic convergence can be attributed to underlying genetic convergence (Gompel and Prud'homme 2009; Christin et al. 2010; Storz 2016). Convergent phenotypes can evolve in unrelated taxa through repeated genetic changes to the same gene family, gene, and even amino acid position (Woods et al. 2006; Castoe et al. 2009; Li et al. 2010; McGlothlin et al. 2014). Highly specific amino acid changes reoccur in protein evolution associated with traits such as insecticide resistance in insects (Dong 2007), high-altitude adapted

hemoglobin in birds (Natarajan et al. 2015), and color vision pigments in vertebrates (Yokoyama and Radlwimmer 2001; Shi and Yokoyama 2003). The prevalence of genetic convergence raises fundamental questions about the repeatability (or “predictability”) of molecular evolution (Weinreich et al. 2006; Stern and Orgogozo 2009). If many conceivable solutions exist to an evolutionary problem, when and why does adaptation proceed through a repeated or predictable route?

Repeated outcomes of molecular evolution are attributed to a number of non-exclusive biases in the substitution process of amino acids, for example, biases toward the few changes that can produce a highly specific phenotypic outcome (Gompel and Prud'homme 2009; Christin et al. 2010) or fixation biases associated with negative pleiotropy (DePristo et al. 2005; Miller

This article corresponds to Kalina T.J.D. (2017), Digest: Know your poison: Predictable molecular changes confer toxin resistance in snakes. *Evolution*. <https://doi.org/10.1111/evo.13259>.

et al. 2006; Weinreich et al. 2006; Tokuriki and Tawfik 2009; Storz 2016). However, it is unclear if convergent outcomes arise through a repeated order of mutational changes. The combinatorial effects of each successive mutation in a series can give rise to nonadditive epistatic properties, in which only a subset of trajectories can achieve a specific outcome (Weinreich et al. 2005, 2006; Bloom et al. 2010; Gong et al. 2013; Natarajan et al. 2016). In extreme examples, certain function-altering mutations are contingent on a specific genetic background where prerequisite (or “permissive”) mutations have already occurred (Ortlund et al. 2007; Blount et al. 2008; Bridgman et al. 2009; Harms and Thornton 2013).

We characterized convergence in the historical order of accumulation of mutations that gave rise to a convergent molecular outcome: tetrodotoxin (TTX) resistance in the skeletal muscle sodium channel (Na_v1.4) of the common garter snake (*T. sirtalis*). In western North American, *T. sirtalis* has evolved resistance to the neurotoxin TTX found in its prey, the Pacific newt (*Taricha* spp.). Arms race coevolution between predator and prey has driven convergent escalation of phenotypic TTX resistance in two separate geographic “hotspots,” central California and the Pacific Northwest (see Fig. 2A; Brodie et al. 2002). Phenotypic convergence in the two hotspots appears to be the result of convergent genetic changes to the Na_v1.4 sodium channel (Geffeney et al. 2005; Brodie and Brodie 2015; Toledo et al. 2016).

TTX binds to the outer pore of voltage-gated sodium (Na_v) channels (Fozzard and Lipkind 2010; Tikhonov and Zhorov 2012), preventing the propagation of action potentials in muscle and nerve tissue. Na_v channels are composed of four homologous domains (DI–DIV), each containing a pore-loop (“p-loop”) that together combine to form the extracellular pore of the channel where TTX binds (Terlau et al. 1991; Fozzard and Lipkind 2010; Payandeh et al. 2011; Tikhonov and Zhorov 2012; Toledo et al. 2016). Geffeney et al. (2005) conducted an initial screen of amino acid variation in the Na_v1.4 pore in TTX-resistant populations of *T. sirtalis*. Domains I, II, and III were found to be invariant, but the DIV p-loop sequence contained three unique, derived alleles (one in California and two in the Pacific Northwest; Fig. 1). Functional expression of these three DIV sequences confirmed that they confer varying levels of TTX resistance to the channel by disrupting TTX-binding at the pore (Geffeney et al. 2005). Channel-level TTX resistance conferred by each DIV allele was also tightly correlated with population differences in muscle and whole-animal levels of resistance (Geffeney et al. 2002, 2005).

To infer the historical order of mutations in the DIV p-loop at each geographic hotspot, we first evaluated variation in Na_v1.4 sequence across populations of *T. sirtalis* throughout western North America. Although the three DIV alleles observed by Geffeney et al. (2005) imply genetic convergence in the two hotspots, these sequences came from an extremely limited sample of only three

wild individuals. In this study, we initially assessed population variation in the full Na_v1.4 coding sequence, then conducted an expanded geographic survey of variation within the DIV p-loop—the only pore region of the channel found to vary among populations. We sought to enumerate all contemporary p-loop variants, including other intermediate or unique combinations of the five identified point mutations (Fig. 1) or other previously unidentified mutations.

Our survey found unique TTX-resistant alleles localized within each geographic hotspot, confirming convergence within the DIV p-loop of the Na_v1.4 channel pore. In both instances, however, TTX-resistant changes to protein structure clearly began with the same Ile-Val change in the DIV p-loop (I1561V; Fig. 1). Next, we generated a gene tree to evaluate if the genealogical history of Na_v1.4 was concordant or discordant with geographic patterns of divergence between the California and Pacific Northwest hotspots. Specifically, we used ancestral sequence reconstruction to test the hypothesis that the I1561V change, which confers a low-to-moderate increase in TTX resistance, evolved independently in each hotspot as an intermediate mutational step towards greater resistance. Sequence reconstruction, combined with contemporary patterns of DIV variation, permitted a comprehensive test of convergence in the historical order of changes in the DIV p-loop at each hotspot.

Methods

SAMPLING SCHEME AND ESTIMATES OF PHENOTYPIC TTX RESISTANCE

To assess patterns of Na_v1.4 variation in populations of *T. sirtalis* throughout western North America and relate genetic variation to phenotypic variation, we used tissue samples from previous work on phenotypic variation in TTX resistance (Brodie et al. 2002; Ridenhour 2004; Feldman et al. 2010). These data were supplemented with additional collections to increase sample size and the geographic scope of our analysis. Our final dataset included 368 individuals sampled from 27 different locations in western North America (Table 1; Fig. 2). We included three sites where *Taricha* do not co-occur with *T. sirtalis* (Feather Lake, Lofton Lake, and Bear Lake) to assess Na_v1.4 variation in the absence of selection from toxic newts.

The following analyses relied predominately on previous population estimates of phenotypic TTX resistance in *T. sirtalis* (Brodie et al. 2002; Ridenhour 2004; Feldman et al. 2010). We scored three additional populations (Carmel Valley, $n = 26$; Feather Lake, $n = 24$; Howard Lake, $n = 4$) for resistance with the same well-established bioassay of whole animal performance used in previous studies (see Fig. S1 and Table S1; Brodie and Brodie 1990; Brodie et al. 2002; Ridenhour et al. 2004). Briefly, each individual was assayed on a 4-m racetrack to characterize

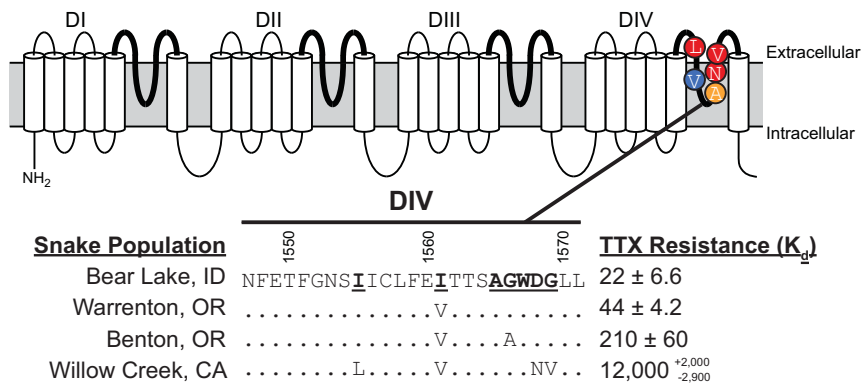


Figure 1. Schematic of the Nav1.4 skeletal muscle sodium channel in *T. sirtalis*. Each domain (DI–IV) is shown above with the extracellular pore loops (p-loops) in solid black lines. Specific amino acid changes in the DIV p-loop are shown in their relative positions in the pore. Below, the ancestral DIV p-loop sequence is listed (collected from Bear Lake, ID), as well as derived changes identified in three other individuals from TTX-resistant populations. The TTX resistance of each allele ($K_d \pm 95\%$ CI) was previously evaluated in cloned Nav1.4 channels, measured as the concentration of TTX (nM) that blocks 50% of cloned channels (Geffeney et al. 2005).

its “baseline” crawl speed, then injected intraperitoneally with a known dose of TTX and assayed for “post-injection” speed. Resistance was estimated as relative performance after injection. Population estimates of TTX resistance are reported on a scale of mass-adjusted mouse units (MAMUs) to adjust for population differences in body size (Brodie et al. 2002). The 50% MAMU dose represents the dose of TTX that reduces the performance of the average snake in a population to 50% of baseline speed. The original data were collected in a manner that precludes estimation of individual-level physiological resistance, so we were able to evaluate population patterns of TTX resistance only (see Brodie et al. 2002).

PRELIMINARY SURVEY OF WHOLE-LOCUS VARIATION IN $NA_V1.4$

The Nav1.4 protein is encoded by *SCN4A*, a 5625 bp gene that consists of 26 exons. Although amino acid variation in the DIV p-loop strongly contributes to phenotypic variation in TTX resistance in western *T. sirtalis* (Geffeney et al. 2005; Feldman et al. 2010), previous studies have not focused on intraspecific variation in other regions of Nav1.4. Amino acid changes to the p-loops of the other three domains (DI–III) have been associated with TTX resistance in other taxa (Brodie and Brodie 2015), including additional species of *Thamnophis* and other snakes (Feldman et al. 2009, 2012), and TTX-bearing species of newts (Hanifin and Gilly 2015) and pufferfish (Jost et al. 2008). Therefore, we chose an initial sample of 20 individuals and sequenced the full protein-coding sequence of *SCN4A*. We sampled two geographically distinct sites, the Bay Area in California ($n = 10$) and Benton, OR ($n = 10$), each located within the hotspots with elevated phenotypic TTX resistance (Brodie et al. 2002).

We extracted genomic DNA using the DNeasy Blood & Tissue kit (Qiagen Inc., Valencia, CA.). We used custom primers to

amplify all 26 exons of *SCN4A* (Fig. S2) and sequenced fragments in both directions on an Applied Biosystems 3730xl DNA Genetic Analyzer at the DNA Analysis Facility at Yale University. We used Geneious 4.8.5 (Biomatters Ltd., Auckland, New Zealand) to align, edit, and translate protein-coding regions, and then we examined functional variation in the four p-loops (DI–DIV). All sequences were deposited in GenBank (KY744954–KY745723).

We also used a number of metrics to assess genetic variation across the full *SCN4A* coding sequence. We estimated levels of nucleotide diversity at synonymous and nonsynonymous sites using Nei’s θ (π ; Watterson 1975; Tajima 1983) and Watterson’s θ (Watterson 1975) in DnaSP 5.10.1 (Librado and Rozas 2009). We used the same program to test for departures from neutral expectations using Tajima’s D (Tajima 1989). We then used pairwise F_{ST} estimates to characterize among-population variation between the California and Oregon sites. We calculated estimates of F_{ST} using the “diveRsity” package in R (Keenan et al. 2013; R Core Team 2016) and estimated 95% confidence intervals with 1000 bootstrap iterations.

EXPANDED SURVEY OF VARIATION IN THE DIV P-LOOP

The initial survey of 20 individuals indicated that the majority of Nav1.4 coding sequence, including the p-loops in Domains I–III, is invariant among populations (see Results section). Therefore, we focused our expanded population survey on the variable DIV p-loop region in our full dataset of 368 individuals from 27 different locations. The DIV p-loop is located approximately in the center of exon 26 of *SCN4A* (McGlothlin et al. 2014). For each individual, we sequenced a 666 bp fragment of exon 26 that included the DIV p-loop region. We identified heterozygous sites by visual inspection in Geneious and confirmed heterozygosity

Table 1. Population estimates of phenotypic TTX resistance and DIV p-loop allele variation.

| Population | County | 50% MAMU Dose | No. of Individuals | N_A | H_O | H_E | F_{IS} | HWE Exact Test |
|----------------------------|---------------------|---------------------|-----------------------|-------|-------|-------|----------|-------------------|
| Bear Lake | Bear Lake, ID | 3.6 | 14 | 1 | – | – | – | – |
| Benton | Benton., OR | 34.1 | 43 | 3 | 0.233 | 0.498 | 0.536 | 0.0002* |
| Carmel Valley [†] | Monterey, CA | 451.0 | 27 | 2 | 0.148 | 0.492 | 0.703 | 0.0003* |
| Clallam | Clallam, WA | 4.5 | 12 | 1 | – | – | – | – |
| Cresecent | Del Norte, CA | 4.2 | 12 | 1 | – | – | – | – |
| Dupont | Pierce, WA | 27.9 | 19 | 2 | 0.158 | 0.508 | 0.695 | 0.0040* |
| East Bay | Contra Costa, CA | 945.1 | 4 | 1 | – | – | – | – |
| Feather Lake [†] | Lassen, CA | 3.1 | 9 | 1 | – | – | – | – |
| Gilroy | Santa Cruz, CA | 18.4 | 33 | 3 | 0.303 | 0.514 | 0.415 | 0.0015* |
| Hoquiam | Grays Harbor, WA | 7.0 | 4 | 2 | 0.000 | 0.429 | 1.000 | 0.1436 |
| Howard Lake [†] | Mendocino, CA | 22.7 | 6 | 1 | – | – | – | – |
| Ledson Marsh | Sonoma, CA | 10.4 | 11 | 2 | 0.455 | 0.506 | 0.107 | 1.0000 |
| Lofton Lake | Lake, OR | 2.2 | 13 | 1 | – | – | – | – |
| Lost Lake | Hood River, OR | 4.6 | 7 | 1 | – | – | – | – |
| Mill City | Marion, OR | 15.9 | 6 | 3 | 0.167 | 0.712 | 0.783 | 0.0132 |
| Omo | El Dorado, CA | 560.0 | 5 | 1 | – | – | – | – |
| Orick | Humboldt, CA | 4.6 | 8 | 1 | – | – | – | – |
| Parsnip | Jackson, OR | 4.7 | 10 | 1 | – | – | – | – |
| Potter's Slough | Pacific, WA | 19.6 | 15 | 3 | 0.267 | 0.674 | 0.613 | 0.0087 |
| Priest Lake | Texada Island, BC | 4.3 | 10 | 1 | – | – | – | – |
| San Simeon | San Luis Obispo, CA | 5.6 | 7 | 2 | 0.000 | 0.264 | 1.000 | 0.0739 |
| Skagit | Skagit, WA | 4.4 | 17 | 1 | – | – | – | – |
| Stayton | Marion, OR | 22.2 | 11 | 3 | 0.091 | 0.602 | 0.855 | 0.0006* |
| Ten Mile | Lane, OR | 52.2 | 7 | 2 | 0.000 | 0.440 | 1.000 | 0.0204 |
| Warrenton | Clatsop, OR | 15.2 | 22 | 3 | 0.045 | 0.210 | 0.788 | 0.0014* |
| Willits | Mendocino, CA | 6.7 | 16 | 2 | 0.063 | 0.175 | 0.651 | 0.0970 |
| Willow Creek | Sonoma, CA | 729.7 | 20 | 2 | 0.000 | 0.185 | 1.000 | 0.0019* |

Population estimates of phenotypic TTX resistance and the number of individuals sampled for each locality are shown. Locations assayed for phenotypic resistance for the first time in this study are marked with a "†". Population genetic estimates of DIV allele variation for each location include the number of unique alleles (N_A), observed heterozygosity (H_O), expected heterozygosity (H_E), the inbreeding coefficient (F_{IS}), and the HWE exact test P -value. Significant values after a Bonferroni correction are indicated with an asterisks (*).

in both directions with sequencing. We inferred gametic phase computationally with the program PHASE (Stephens et al. 2001) and recovered gametic phase above a 90% confidence threshold for all but two individuals.

To assess functional variation in the DIV p-loop in relation to TTX resistance, we translated the exon 26 coding sequence and scored unique alleles based on amino acid sequence of the DIV p-loop where TTX binds (e.g., those shown in Fig. 1). For each sampling location, we calculated the number of unique alleles (N_A), observed heterozygosity (H_O), and expected heterozygosity (H_E) in Arlequin 3.5 (Excoffier and Lischer 2010). We estimated inbreeding coefficients (F_{IS}) and tested for deviations from Hardy-Weinberg equilibrium (HWE) using exact tests in GenePop v4 (Raymond and Rousset 1995; Rousset 2008). We estimated P -values with the Markov chain method, running 100 batches and

2000 iterations per batch, then adjusted P -values with a sequential Bonferroni correction (Holm 1979). As a preliminary estimate of the evolutionary relationship among DIV alleles, we used the 666 bp of coding sequence to generate a TCS parsimony haplotype network (Templeton et al. 1992; Clement et al. 2000) implemented in the program PopART (Leigh and Bryant 2015).

If amino acid variation in the DIV p-loop explains phenotypic variation in TTX resistance, then we expect populations with a high frequency of TTX-resistant DIV alleles to also have high estimates of phenotypic TTX resistance. We used a nonparametric Spearman's rank correlation test (r_S) to test for a relationship between population patterns of DIV variation and phenotypic TTX resistance. Specifically, we tested for a correlation between a population's cumulative frequency of all TTX-resistant DIV alleles and its estimate of phenotypic TTX resistance. We used

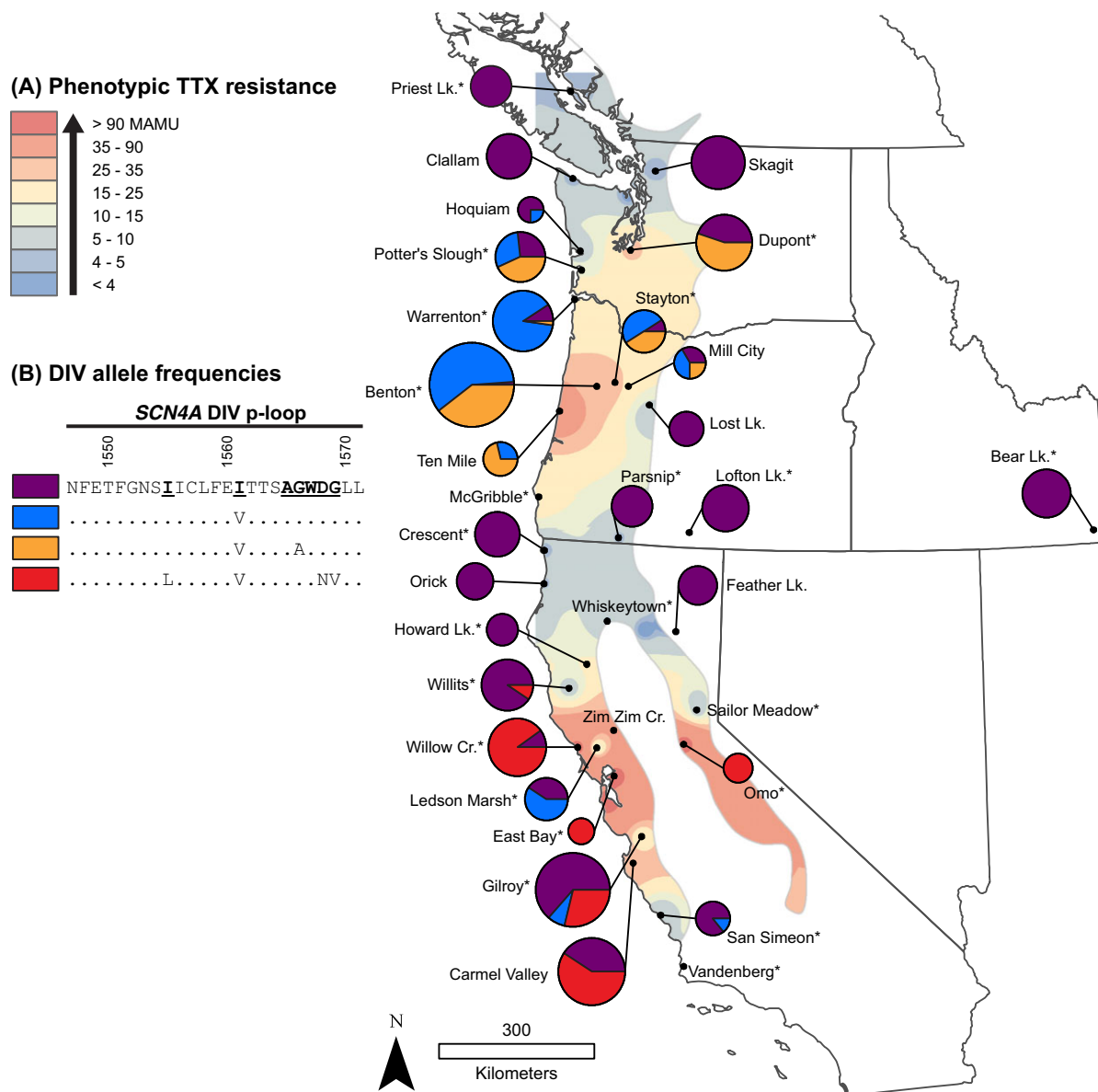


Figure 2. (A) Average phenotypic TTX resistance (50% MAMU) in populations of *T. sirtalis* in western North America. Estimates are interpolated across the geographic range wherein *T. sirtalis* occur in sympatry with *Taricha* newts (recreated from Brodie et al. 2002). (B) Pie charts indicate observed population frequencies of the four unique DIV alleles identified in this study. Chart size is proportional to the sample size at each location. All localities used in the phylogenetic analysis are marked with an asterisk (*).

ArcMap 10.3 (ESRI Inc., Redlands, CA) to visualize population patterns of allele variation and phenotypic TTX resistance.

HISTORICAL ANALYSIS OF THE DIV P-LOOP

We generated a *SCN4A* gene tree to characterize the evolutionary history of the Na_v1.4 channel in western *T. sirtalis*. We selected a subset of 40 individuals from our collection that represent (1) a broad geographic sample of western North America and (2) a representative sample of all unique DIV alleles identified in the preceding analysis. We did our best to include a thorough distribution of localities and DIV alleles throughout the range

of western *T. sirtalis* to avoid biasing a particular geographic region or DIV sequence in our analysis. We then included four individuals from central and eastern North America and used two sister taxa, the western ribbon snake (*Thamnophis proximus*) and eastern ribbon snake (*Thamnophis sauritus*), as outgroups.

We used *SCN4A* sequence data in our phylogenetic analysis of Na_v1.4 (rather than unlinked neutral markers) to limit potential issues with hemiplasy—the incorrect inference of genetic convergence due to incomplete lineage sorting and gene tree-species tree discordance (see Storz 2016). We used 666 bp from the previous analysis, combined with another primer pair, to sequence

the majority of exon 26 (1144 bp), the final exon at the 3' end of *SCN4A* protein-coding sequence that includes the DIV p-loop (McGlothlin et al. 2014). Because most of the *SCN4A* coding sequence lacked sufficient variation for a phylogenetic analysis, we used walking primers to sequence a 3606 bp fragment of non-coding sequence to the immediate 3' flank of exon 26 (Fig. S2). We focused our analysis on this 3' non-coding region because it is tightly linked to the DIV p-loop in exon 26. Assuming recombination has not occurred, sequence variation in the 3' flank should reflect the genealogical history of the DIV p-loop. Phylogenetic analyses assume no recombination, and recombinants can confound inference when they contain merged haplotypes from different evolutionary histories. Given the tight proximity of the DIV p-loop and the 3' flanking fragment, we did not anticipate recombination problems in our dataset. As a precaution, we implemented a suite of recombination tests in the program PhiPack (Jakobsen and Easteal 1996; Smith and Smith 2002; Bruen et al. 2006).

In our sample of western *T. sirtalis*, we avoided heterozygous individuals to limit problems with null alleles and the resolution of gametic phases among primer pairs along the 3' flank. The group of 40 western *T. sirtalis* contained only four heterozygous individuals, and of all polymorphic sites in the alignment, a proportion of 0.225 was heterozygous. For the following analyses, the heterozygous sites of these four individuals were coded as ambiguities. None of the individuals in the final alignment contained heterozygous sites in the DIV p-loop. We collapsed redundant sequences in the alignment if they were found within the same locality, but retained redundancies if they were found in multiple sampling locations. The final concatenated alignment of exon 26 (1144 bp) and its 3' flank (3606 bp) contained a total of 4750 bp. The exon 26 fragment had 22 polymorphic sites (proportion informative = 0.68), and the 3' flanking fragment had 123 polymorphic sites (proportion informative = 0.66).

To account for potential differences in patterns of evolution among loci, we conducted a partitioned phylogenetic analysis and estimated separate substitution models for the exon 26 coding and 3' non-coding fragments (e.g., Castoe and Parkinson 2006; McGuire et al. 2007; Brown et al. 2009). We used JModelTest 2.1.7 (Guindon and Gascuel 2003; Darriba et al. 2012) to select the best-fit DNA substitution models for exon 26 (HKY85) and the 3' fragment (HKY85 + I). We conducted the partitioned phylogenetic analysis using Bayesian inference (BI) in the program MrBayes 3.2 (Ronquist et al. 2012). The program implemented the separate substitution models for each partition and also allowed for among-partition variation in evolutionary rates, which has been shown to improve branch length estimation (Marshall et al. 2006). Four simultaneous runs with six heated chains for 10,000,000 generations were performed, saving every 1000th generation. We set the burn-in to 25,000 samples and then used the

remaining samples to generate the final majority consensus tree and posterior probabilities. We confirmed stationarity in the program Tracer 1.6 by comparing fluctuating values of the likelihood from the four independent searches (Rambaut et al. 2014). We also estimated the phylogeny with a partitioned maximum likelihood (ML) analysis in RAxML 8.2.4 (Stamatakis 2014). The current version of RAxML does not allow the application of different substitution models in partitioned analyses, so we implemented the HKY + I model for both exon 26 and the 3' non-coding fragments. RAxML also only allows for optimization of a single evolutionary rate across all partitions. We estimated branch support with 1000 nonparametric bootstrap replicates. The BI and ML analyses produced identical topologies, which we visualized in the program TreeGraph2 (Stöver and Müller 2010).

We took two precautions to assess the robustness of our partitioning strategy. First, we compared these partitioned results to analogous analyses with unpartitioned data. Accounting for coding and non-coding regions in the partitioned analyses appeared to have little effect, as the partitioned and unpartitioned data produced the same tree topology. Second, to assess whether the putative convergent site in the DIV p-loop of exon 26 (I1561V) might bias results, we removed exon 26 from the alignment and reran the entire analysis with only 3606 bp of 3' non-coding sequence (Fig. S4).

To further assess patterns of population structure at the *SCN4A* locus, we analyzed the full dataset in the population genetic program BAPS 6.0 (Corander et al. 2008), which allows for admixture within and among lineages. We used the sequence data from all 40 western *T. sirtalis* to infer the optimal number of genetic groupings (k) without prior information of sampling locations. First, we ran the analysis assuming a mixture model to determine the most probable k . We set k to a maximum of 23, the total number of different western sampling sites in the dataset. The resulting mixture clusters were used for the admixture analysis. We used recommended admixture settings, including 200 reference individuals, and we repeated the analysis 100 times per individual. The entire analysis was repeated five times to check for convergence among different runs.

Lastly, we sought to reconstruct the historical order of substitutions to the DIV p-loop of Na_v1.4 in the California and Pacific Northwest hotspots. We used the *SCN4A* gene tree topology and branch lengths to reconstruct the DIV p-loop amino acid sequences of ancestral nodes using an ML approach implemented in the program PAML 4.9 (Yang 2007). We used the same program to calculate marginal posterior probabilities, which represent the likelihood that a correct amino acid was reconstructed at a given site under the model's assumptions. We inferred ancestral DIV p-loop sequences using three different forms of ML models (amino acid-, codon-, and nucleotide-based), and then assessed congruence across the reconstructions (see Chang et al. 2002).

Contemporary patterns of DIV variation suggested the same I1561V change evolved independently in the two separate hotspots as an initial mutational step towards more TTX-resistant changes (see Results section, Fig. 2). We used a likelihood-based Shimodaira–Hasegawa test (Shimodaira and Hasegawa 1999) to test the *a priori* null hypothesis that the I1561V change instead arose only once. To do so, we generated a second ML tree where all taxa with the I1561V change (from both California and the Pacific Northwest) were constrained to monophyly. We used the SH-test to compare fit of the constraint tree to that of our original unconstrained ML tree. We assessed significance with 10,000 bootstrap replicates in the package “phangorn” in R (Schliep 2011).

Results

CONTEMPORARY VARIATION IN $Na_v1.4$

Population variation in the full $Na_v1.4$ protein-coding sequence of *T. sirtalis* was limited almost entirely to the DIV p-loop region. Overall nucleotide variation in the full 5625 bp of *SCN4A* sequence was low for both synonymous (Bay Area, $\pi < 0.0001$; Benton $\pi = 0.0014$) and nonsynonymous sites (Bay Area, $\pi = 0.0003$; Benton $\pi = 0.0002$; Table S2). Tajima’s *D* values for the full sequence were negative for both the Bay Area and Benton samples, although not significant. Sliding window analyses of Tajima’s *D* with varying window sizes revealed a similar pattern (data not shown). We found only six polymorphic amino acid positions in the full translated sequence, all of which varied both within- and among-populations (Fig. S3). Five of the six sites were the specific point mutations previously associated with TTX resistance in the DIV p-loop (i.e., those in Fig. 1). The sixth site was located at amino acid position 549 in the intracellular portion of the protein, outside of the pore region (nonsynonymous position 1654 bp in Fig. S3). We found no evidence of variation in the p-loops of domains I–III.

Our expanded geographic sample of the DIV p-loop sequence uncovered both within- and among-population variation in the three derived alleles characterized previously by Geffeney et al. (2005) (Fig. 2). The five known point mutations to the DIV p-loop occurred only in these three specific combinations. We did not find other intermediate or unique alleles, nor other novel mutations to the p-loop. Population variation in the three derived alleles was also consistent with geographic patterns of phenotypic TTX resistance. Observed frequencies of TTX-resistant alleles were tightly correlated with population estimates of phenotypic TTX resistance (Fig. 3, Spearman’s rank correlation, $r_s = 0.848$, $P < 0.001$), and the occurrence of TTX-resistant alleles was localized within the two hotspots. Allele frequencies were consistently out of HWE, as expected for a locus under strong selection (Table 1).

We generated a parsimony haplotype network for 286 individuals from which we were able to sequence the full 666 bp

fragment of coding sequencing in exon 26 (Fig. 4 inset). The parsimony network was largely uninformative because almost all the polymorphic sites in the alignment were the nonsynonymous changes in the p-loop that confer TTX resistance. Consequently, taxa grouped according to their specific DIV p-loop amino acid sequence. Despite low divergence in the protein-coding sequence, haplotypes in the network did fall into two apparent geographic groups, a California/Northwest Coast and an Intermountain group. This broad pattern of divergence was also reflected in the phylogenetic analysis (see next).

HISTORICAL ANALYSIS OF THE DIV P-LOOP

Tests for signatures of recombination (PHI, NSS, and Max χ^2) were nonsignificant for our sample of western *T. sirtalis*, so we proceeded with the phylogenetic analysis. The partitioned BI and ML *SCN4A* gene trees of the full 4750 bp dataset broadly supported three geographic clades within western *T. sirtalis*: (1) central California, (2) the Northwest Coast, and (3) an Intermountain clade that spanned the Cascade and Klamath mountain ranges (Fig. 4). Each of the three groups had a posterior probability >0.95 and bootstrap support >70 in the BI and ML analyses, respectively. The analysis of the reduced dataset (excluding the 1144 bp exon 26 fragment) produced the same three well-supported clades, but lacked the same resolution among DIV alleles within each geographic group (Fig. S4).

The population genetic BAPS analysis identified four genetic clusters ($k = 4$, Fig. 4) as the most likely number of groupings, which were consistent with geographic patterns in the phylogeny. All individuals had posterior admixture coefficients >0.85 , and no individuals showed evidence for admixture exceeding the threshold of $P = 0.05$. BAPS results were consistent across all five replicate runs. Individuals from the Northwest Coast and Intermountain clades formed two separate genetic groups, as in the phylogeny. The analysis did detect additional structure among DIV alleles in California, where all individuals with the ancestral sequence or I1561V change formed one group and individuals with the additional changes I1555L, D1568N, and G1569V formed a second group.

The gene tree topology supported two independent origins of the I1561V change in the California and Northwest Coast clades. The two parallel changes were intermediate steps to more TTX-resistant, but unique, DIV alleles in each of the two lineages. The ancestral sequence reconstruction in PAML also supported this evolutionary history (Fig. 4). Results from the amino acid-, codon-, and nucleotide-based models were all congruent, and all ancestral nodes were supported with posterior probabilities >0.99 . Finally, the topology of our best ML tree was a significantly better fit than the constraint tree where all I1561V taxa were forced into monophyly (SH test, $P = 0.0187$).

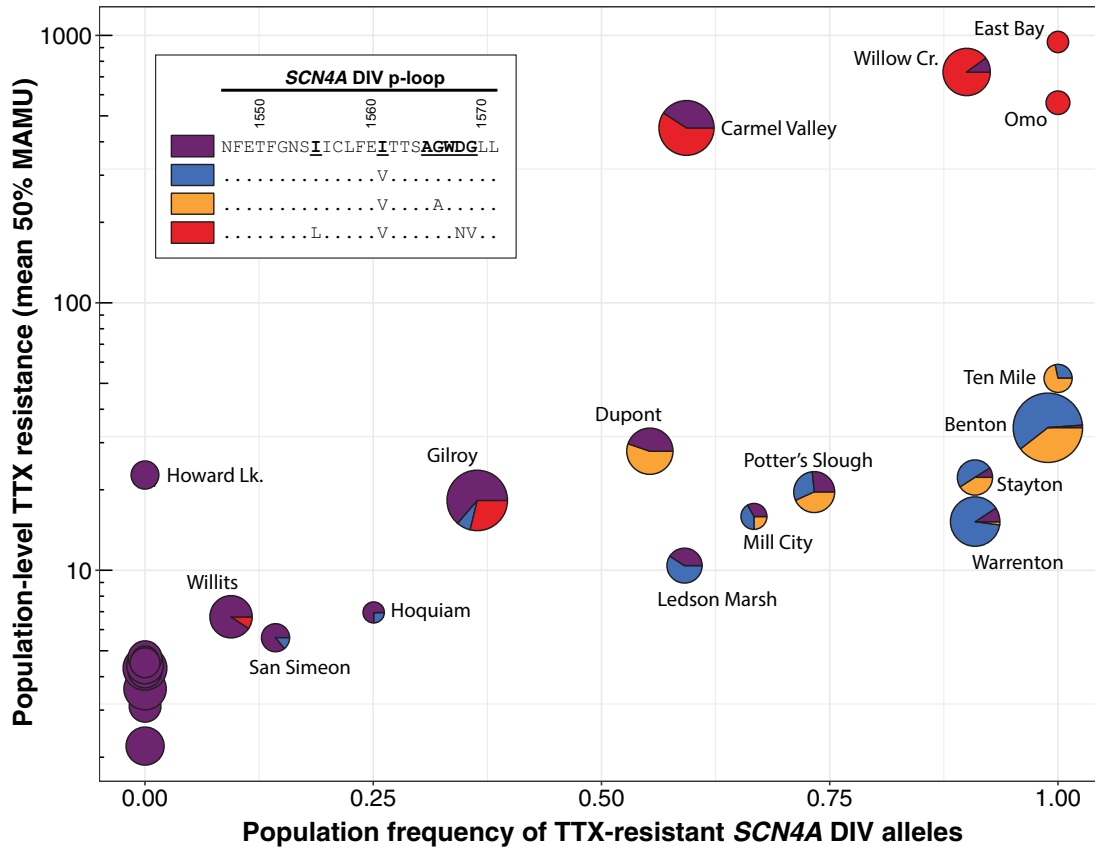


Figure 3. Relationship between the frequency of TTX-resistant DIV alleles and the phenotypic TTX resistance (50% MAMU) of each population. Each locality is represented by its pie chart from Figure 2. All alleles that differ from the ancestral DIV sequence have been demonstrated to be TTX resistant. All unlabeled localities clustered in the lower left-hand corner have <5 MAMU estimates of TTX resistance.

Discussion

Contemporary patterns of variation in western *T. sirtalis* suggest the evolution of TTX-resistant mutations in Na_v1.4 proceeded independently in two separate lineages, yet began with the same first mutational step. An I1561V change in the DIV p-loop likely arose independently in each of the two geographic hotspots of elevated phenotypic TTX resistance. This initial mutation was followed by a small number of unique, lineage-specific changes to the DIV p-loop in each hotspot. Below, we discuss evidence for historical convergence and then potential drivers of repeated change to the DIV p-loop.

HISTORICAL CONVERGENCE IN THE DIV P-LOOP

Patterns of population variation in the Na_v1.4 channel demonstrate that TTX-resistant mutations in the DIV p-loop evolved independently in two separate geographic regions. The I1561V allele was found in both hotspots; however, the I1555L-D1568N-G1569V allele was unique to California and the G1566A allele unique to the Pacific Northwest. Population frequencies of these three TTX-resistant DIV alleles were tightly correlated with

population mean estimates of phenotypic TTX resistance throughout western North America (Figs. 2 and 3). Outside the two hotspots, we only found the ancestral Na_v1.4 sequence. For example, non-resistant populations located between the two hotspots (Crescent and Parsnip) and in allopatry with *Taricha* newts (Lofton Lake and Bear Lake) were fixed for the ancestral DIV amino acid sequence.

Contemporary patterns of allelic variation provide strong evidence that TTX-resistant mutations in the DIV p-loop began with the same I1561V change in each hotspot. The I1561V change is the only point mutation to occur in *all* derived alleles in both hotspots. Prior to this study, the I1561V allele (which confers a slight increase in TTX resistance) was not known to occur in California; however, we detected the allele in both hotspots. In our sample, the other point mutations in the two highly resistant alleles (I1555L-D1568N-G1569V in California; G1566A in the Pacific Northwest) never occurred in lineages without the initial I1561V change. Our wide-ranging survey of 368 individuals from 27 localities did not uncover other intermediate or unique mutational combinations that lacked the I1561V change.

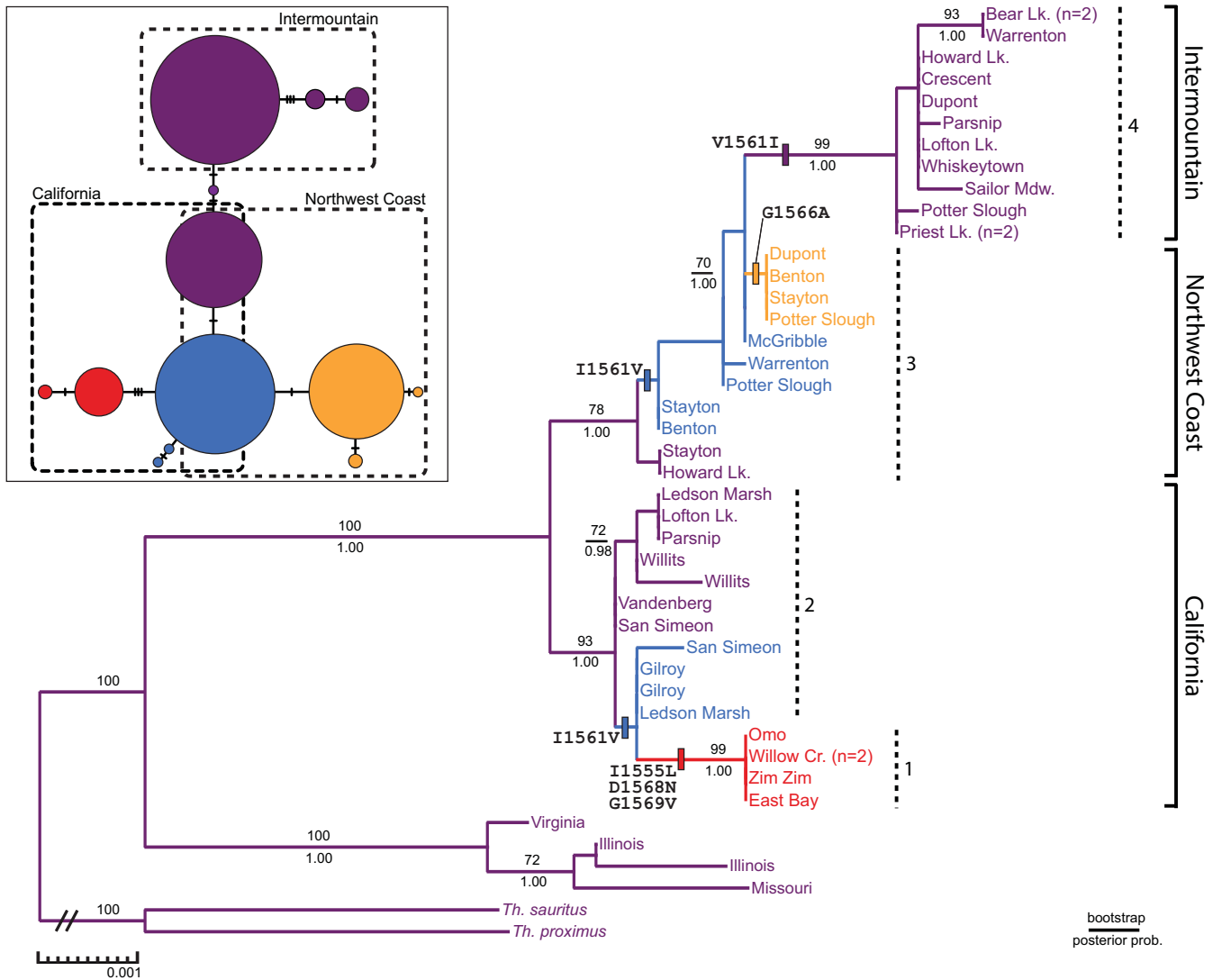


Figure 4. Evolutionary relationships among DIV sequences. Inset shows the haplotype network of 666 bp of exon 26 protein-coding sequence that includes the DIV p-loop. Circles represent unique observed haplotypes with size proportional to their frequency in the sample. Intermediate mutational steps are represented by dashes along the lines connecting haplotypes. Each haplotype is color-coded by its DIV p-loop amino acid sequence, as shown in Figure 2. Approximate geographic groupings are shown with dashed boxes. Below, the *SCN4A* gene tree is shown with ML bootstrap support and BI posterior probabilities. Each individual taxon is labeled according to its sampling location and color-coded by its DIV p-loop sequence. Branches are labeled to reflect the identify of mutational changes from the PAML ancestral sequence reconstruction of the DIV p-loop. Vertical dashed lines to the right of taxa (labeled 1–4) identify the four genetic groups from the BAPS analysis.

The *SCN4A* gene tree also indicated the I1561V change was the first mutation to arise in each hotspot (Fig. 4). In the phylogeny, taxa sampled from the California and Pacific Northwest hotspots generally grouped within the California and Northwest Coast clades, respectively. Within each of these clades, the I1561V change was the initial mutational step towards TTX resistance, preceding the other point mutations in alleles that confer higher resistance. In addition, the phylogenetic analysis suggested the I1561V changes found in each hotspot are not identical-by-descent, but rather arose independently. Two separate I1561V

changes were also supported by the ancestral sequence reconstruction, an analysis that is considered robust despite phylogenetic uncertainty (Hanson-Smith et al. 2010) and when divergence is low (Zhang and Nei 1997; Blanchette et al. 2004). The constraint tree (with forced monophyly of all I1561V taxa) was significantly less likely than our best ML topology that depicted two I1561V changes.

The three geographic groups identified from the gene tree and BAPS analysis (California, Northwest Coast, and Intermountain) were qualitatively similar to those in an mtDNA phylogeny

of western *T. sirtalis* by Janzen et al. (2002), highlighting the need to interpret $N_{AV}1.4$ evolution in the context of historical biogeography. The mtDNA tree supported a pattern of post-glacial population expansion in the last ~10,000 years from two separate glacial refugia: (1) a northward population expansion out of southern California and (2) a southward expansion from southwestern Canada. Populations in the two hotspots, where the I1561V changes putatively arose in parallel, appeared genetically disparate in the mtDNA phylogeny. As in the *SCN4A* tree, Janzen et al. (2002) found divergence between populations in California and the Pacific Northwest. The intersecting mountain ranges at the California-Oregon border, located between the two hotspots, are a site of historical vicariance for not only *T. sirtalis*, but also many other co-distributed taxa (Mahoney 2004; Mead et al. 2005; Swenson et al. 2005), including the newt *Taricha granulosa* (Kuchta and Tan 2005). This pattern of north-south divergence might help explain how genetic convergence arose if populations in California and the Northwest were historically isolated. Historical vicariance may also explain why a number of localities in our *SCN4A* gene tree contained individuals that grouped into multiple geographic clades (e.g., Howard Lake grouped in both the California and Northwest Coast clades). A number of these localities lie in regions that appear to have been influenced by vicariance (e.g., Howard Lake located in the Northern Coast Range of California) and may now represent contact zones between the three geographic clades (Janzen et al. 2002).

Although our phylogenetic analysis provides evidence for parallel, independent I1561V changes in the two hotspots, we cannot rule out alternative scenarios. We consider recombination an unlikely explanation because the 3' non-coding sequence used in the gene tree is closely linked to the DIV p-loop, and tests for recombination were nonsignificant. However, a more comprehensive test for recombination would involve evaluating sequence variation on both sides of the DIV p-loop, not just the 3' flanking region. A more plausible alternative may be the retention of an undetected ancestral polymorphism (e.g., Colosimo et al. 2005; Barrett and Schluter 2008). A polymorphism at position 1561 could have existed at low frequency in the ancestor of western *T. sirtalis*, with the I1561V change subsequently increasing due to contemporary selection in each of the two hotspots. In addition, our phylogenetic analysis of the reduced dataset (excluding exon 26 and the putatively convergent I1561V site) was ambiguous to whether the I1561V change arose twice or existed as an ancestral polymorphism (Fig. S4). Retention of polymorphisms and incomplete lineage sorting could also help explain why certain localities in the *SCN4A* gene tree contained individuals that grouped in multiple geographic clades (e.g., Howard Lake).

Unfortunately, nucleotide variation in the DIV p-loop does not help to distinguish between convergence and ancestral polymorphism at the amino acid level. In the standard genetic code,

the adenine-guanine mutation found in both hotspots is the only single point mutation in a codon triplet capable of generating an isoleucine-valine amino acid change. The scope of this study does not permit genome-spanning estimates of linkage disequilibrium to elucidate signatures of selection (Innan and Kim 2004; Prezeworski et al. 2005); however, an ancestral I1561V polymorphism may be less probable given contemporary patterns of DIV variation. We surveyed a total of 111 individuals from 10 populations with low phenotypic resistance surrounding the hotspots—including five sites located between the two hotspots—and did not find evidence of the I1561V allele (Fig. 2). Moreover, the I1561V change has never been found in eastern populations of *T. sirtalis* (Feldman et al. 2009; Avila 2015), which are ancestral to the California and Northwest Coast clades in our *SCN4A* phylogeny, or in other TTX-resistant *Thamnophis* species (Feldman et al. 2009, 2012; McGlothlin et al. 2016).

POTENTIAL DRIVERS OF HISTORICAL CONVERGENCE

Convergent evolution at the protein level generally occurs for two non-exclusive reasons (reviewed in Storz 2016). In some cases, only a limited number of mutations can produce a specific phenotypic outcome. For example, the target of selection may be highly specific and changes to only a few specialized loci can produce a requisite outcome (Gompel and Prud'homme 2009; Stern and Orgogozo 2009; Christin et al. 2010; Storz 2016). TTX resistance has repeatedly evolved in a number of unrelated taxa through specific genetic changes to the $N_{AV}1.4$ pore that disrupt TTX-binding (Jost et al. 2008; Feldman et al. 2009, 2012; Brodie and Brodie 2015; Hanifin and Gilly 2015; Toledo et al. 2016). Genetic convergence in the DIV p-loop of *T. sirtalis* (and other taxa) must be due in part to the specificity of toxin binding—only a subset of residues in the four p-loops actually interact with TTX (Fozzard and Lipkind 2010; Tikhonov and Zhorov 2012). However, it seems unlikely that binding specificity alone can explain convergence in the historical order of changes to the DIV p-loop.

Convergence can also arise due to different forms of substitution biases that influence which amino acid changes contribute to phenotypic variation. Mutational biases, like transition:transversion rates, may affect the direction of molecular evolution (Yampolsky and Stoltzfus 2001; Stoltzfus and Yampolsky 2009; Storz 2016); however, recent work has focused on fixation biases and negative pleiotropy. Certain beneficial mutations may be unlikely to persist due to pleiotropic effects that disrupt some other aspect of protein structure or function. Pleiotropy can bias the identity and position of mutations, but also the number of feasible mutational routes to an adaptive phenotype (DePristo et al. 2005; Miller et al. 2006; Weinreich et al. 2006; Tokuriki and Tawfik 2009; Feldman et al. 2012; Storz 2016). Epistatic effects arise through the combinatorial interactions of each successive

mutation and its predecessors, so the consequences of each mutational step depend on its current genetic background (Weinreich et al. 2005, 2006; Poelwijk et al. 2007; Bank et al. 2016; Natarajan et al. 2016; Storz 2016). Thus, the overall effect of a series of mutations may depend on the sequential order in which they occur. For example, certain function-altering changes are contingent on a genetic background where other requisite or permissive mutations have already occurred (Ortlund et al. 2007; Blount et al. 2008; Bridgham et al. 2009; Harms and Thornton 2013; Storz 2016).

Changes to the $\text{Na}_V1.4$ pore probably reflect a delicate balance between TTX-resistant properties and the maintenance of Na_V channel function (Feldman et al. 2012; Toledo et al. 2016). Na_V channels play the highly conserved role of signaling in muscle and nerve tissue (Goldin 2002). We found a lack of polymorphism and negative Tajima's D values in the full *SCN4A* coding sequence (Table S2 and Fig. S3), which are consistent with a history of purifying selection on the $\text{Na}_V1.4$ channel. In particular, the p-loops of Na_V channels are highly conserved among vertebrates (Tikhonov and Zhorov 2005; Brodie and Brodie 2015). The p-loops form the selectivity filter at the channel pore, which is critically responsible for the selective influx of Na^+ ions that propagate action potentials. Many of these amino acid residues in the filter also interact with TTX (Fozzard and Lipkind 2010), and TTX-resistant changes to the p-loops can compromise signaling properties of the channel by disrupting Na^+ conductance (Terlau et al. 1991; Feldman et al. 2012) and increasing calcium ion permeability (Heinemann et al. 1992). Consequently, only a limited number of mutations can confer TTX resistance without disrupting Na_V ion channel function (Feldman et al. 2012; Toledo et al. 2016).

In western *T. sirtalis*, the I1561V change was clearly the first mutational step towards TTX resistance in both hotspots (regardless of whether the changes are identical-by-state or identical-by-descent). Other point mutations in highly resistant alleles appear to be contingent on the I1561V change, because they always occur in combination. Alone, the I1561V change only provides a slight increase in resistance (Geffeney et al. 2005), and amino acid position 1561 is not thought to directly interact with TTX (Fozzard and Lipkind 2010). However, the Ile-Val change could modify pore structure in a way that disrupts interactions between TTX and other pore residues (Tikhonov and Zhorov 2011; Toledo et al. 2016). It could also represent a permissible intermediate step towards resistance, which enables other mutations that would otherwise disrupt channel function (e.g., Ortlund et al. 2007). Unfortunately, the individual and combinatorial effects of changes in the DIV p-loop have not been functionally evaluated.

Evidence from the Na_V channels of other TTX-resistant taxa implies that amino acid position 1561 does play an important

role in the mutational order of changes to the channel pore. For example, a Thr-Ser change at the homologous position in the $\text{Na}_V1.4$ channel of toxic newt species is associated with TTX resistance. This change is apparently ancestral to all newts (family: Salamandridae) and preceded three other amino acid changes to the DIV p-loop that confer even greater resistance to toxic modern newts (Hanifin and Gilly 2015). Pufferfish in the genus *Arothron* have an Ile-Met change at the homologous position in the $\text{Na}_V1.4a$ channel (teleost fish have two $\text{Na}_V1.4$ paralogs due to an ancient genome duplication; Jost et al. 2008). In *T. sirtalis*, the $\text{Na}_V1.6$ paralog expressed in the peripheral nervous system (PNS) has an identical Ile-Val change at the same position, which apparently arose in parallel with $\text{Na}_V1.4$ and not due to gene conversion. This change probably confers low levels of TTX resistance to PNS channels, but the substitution is ancestral to all Natricines and may not have initially evolved in response to TTX (McGlothlin et al. 2014, 2016).

EVOLUTIONARY LOSS OF TTX RESISTANCE?

Our phylogenetic analysis indicated an unexpected evolutionary loss of TTX resistance in the Intermountain clade (Fig. 4). If TTX-resistant changes to the DIV p-loop do have detrimental pleiotropic effects in the pore, selection could conceivably favor a loss in populations of *T. sirtalis* that occur in allopatry with toxic newts. Lee et al. (2011) used a cloned mammalian $\text{Na}_V1.4$ channel to assess functional consequences of the single I1561V change and the highly resistant California allele (I1561V plus I1555L, D1568N, and G1569V) in the DIV p-loop. Both alleles resulted in a shift in the voltage dependence of slow inactivation, which could ultimately cause an increase in cell excitability. But, it is unclear if such shifts in biophysical properties actually perturb channel function or translate into fitness costs at the organismal level. Brodie and Brodie (1999) found preliminary evidence for a trade-off between whole-animal TTX resistance and crawl speed in *T. sirtalis* from the Pacific Northwest (where we found TTX-resistant DIV alleles). In our sample, we found a recurrent pattern of heterozygote deficiency and high F_{IS} values in the DIV p-loop of many populations (Table 1), which could reflect selection for distinctly resistant and non-resistant genotypes.

The *SCN4A* gene tree may accurately reflect an evolutionary loss of TTX resistance, but we address two other alternatives. Due to the high proportion of TTX-resistant individuals on the Northwest coast (e.g., Ten Mile and Benton), we found few homozygous individuals with the ancestral DIV sequence (unlike the California hotspot, e.g., Willow Creek). More dense taxon sampling, focused on individuals with the ancestral DIV sequence, could help improve phylogenetic resolution and sequence reconstruction in the Pacific Northwest (i.e., Hillis 1998; Hanson-Smith et al. 2010). For example, the tree topology could erroneously

portray a loss of TTX resistance because our sample did not include genotypes that help root the Intermountain clade to ancestral individuals at the base of the Northwest Coast clade. In an alternative scenario, if evolutionary loss of TTX resistance is possible, the I1561V mutation could have instead evolved once in the ancestor of all western *T. sirtalis*, but then was lost twice in the California and Northwest Coast clades. Future studies should assess the potential for an evolutionary loss of resistance in the Na_v1.4 channel.

Conclusion

Evolution is ultimately dependent on the input of novel genetic variation, but the mutations that actually contribute to adaptation may be biased toward a predictable subset of possible alternatives. In *T. sirtalis*, convergent genetic evolution of TTX resistance in the Na_v1.4 channel pore proceeded through the same mutational first step, an I1561V change that apparently arose twice in the separate hotspots. This repeated first step implies that molecular evolution in the Na_v1.4 channel follows a predictable set of rules, wherein an outcome of TTX resistance cannot be achieved unless mutations occur in a particular order within the DIV p-loop. Evolution is of course not entirely deterministic, as we also found unique point mutations in each hotspot.

A growing list of empirical studies point to the importance of sequential order in the mutational route to adaptation. Increasingly, context-dependent effects and intragenic epistasis are recognized as pervasive forces in protein evolution (Weinreich et al. 2005, 2006; Poelwijk et al. 2007; Breen et al. 2012; Natarajan et al. 2013; Storz 2016). For example, in experimental evolution of antibiotic resistance in *E. coli*, the functional consequences of first-step mutations were strong determinants of the identity and order of subsequent adaptive substitutions (Salverda et al. 2011). In vertebrate glucocorticoid receptors, the eventual evolution of cortisol specificity depended on early permissive mutations with characteristic biophysical properties (Ortlund et al. 2007; Bridgham et al. 2009; Harms and Thornton 2014). Thus, the overall “predictability” of molecular evolution may ultimately depend on patterns of contingency and epistasis that determine the identity and order of amino acid substitutions (DePristo et al. 2005; Miller et al. 2006; Weinreich et al. 2006; Tokuriki and Tawfik 2009).

In extreme cases, sign epistasis can cause a single substitution to have opposing functional or fitness consequences in different genetic backgrounds (Weinreich et al. 2005; Harms and Thornton 2013; Shah et al. 2015; Storz 2016; Ono et al. 2017). Unlike our results, Natarajan et al. (2015, 2016) found that convergence in hemoglobin-oxygen affinity in high-altitude avian species did not evolve through a repeated order of mutations to hemoglobin. However, functional analysis showed that the effects

of individual mutations were still dependent on their genetic background. Molecular evolution was therefore unpredictable due to lineage-specific patterns of intragenic epistasis. On the other hand, closely related taxa are predicted to share similar genetic and developmental constraints due to their common genetic background (Wake 1991; Arthur 2001; Yoon and Baum 2004; Losos 2011). If mutations do exhibit context-dependent effects, then protein evolution may be most predictable in closely related organisms, such as populations of *T. sirtalis* that share a very similar Na_v1.4 protein sequence. Although molecular evolution is deterministic in both examples, hemoglobin and the Na_v1.4 channel, change may only be “predictable” in organisms that share similar genetic backgrounds.

AUTHOR CONTRIBUTIONS

MTJH designed the project, collected genetic data, and performed analyses. CRF collected genetic and phenotypic data, and helped with analyses. EDB Jr. collected phenotypic data and provided leadership on the project. EDB III designed the project, collected phenotypic data, and provided leadership. All authors prepared the manuscript.

ACKNOWLEDGMENTS

This work was supported by a Rosemary Grant Award from the Society for the Study of Evolution, a Grant-in-Aid of Research from the Society for Integrative and Comparative Biology, a Theodore Roosevelt Memorial Grant from the American Museum of Natural History, and a Doctoral Dissertation Improvement Grant from the National Science Foundation (DEB 1601296) to MTJH and EDB III, as well as NSF awards to EDB III and EDB Jr. (DEB 0922216) and to CRF (IOS 1355221). We thank CAF&W for the scientific collecting permit (SC-000814 to CRF) and IACUCs for protocols to EDB Jr. at USU (1008) and CRF at UNR (00453 and 00687). We also thank C. Alencar and E. Ely for curating our *T. sirtalis* tissue collections, and A. Mortensen, J. Scoville, A. Wilkinson, and G. Blaustein for aid with captive animal care. We thank J. McGlothlin for help with primer design. Members of the E. Brodie and R. Cox labs at the University of Virginia provided helpful comments that improved this manuscript. The authors declare no conflict of interest.

DATA ARCHIVING

DNA sequence alignments are deposited in GenBank (KY744954-KY745723). All other data are available through Dryad (DOI: 10.5061/dryad.3k15h).

LITERATURE CITED

- Arthur, W. 2001. Developmental drive: an important determinant of the direction of phenotypic evolution. *Evol. Dev.* 3:271–278.
- Avila, L. A. 2015. Feeding ecology and tetrodotoxin resistance in Eastern *Thamnophis sirtalis*. Doctoral diss., University of Virginia, Charlottesville, VA.
- Bank, C., S. Matuszewski, R. T. Hietpas, and J. D. Jensen. 2016. On the (un)predictability of a large intragenic fitness landscape. *Proc. Natl. Acad. Sci.* 113:14085–14090.
- Barrett, R. D. H., and D. Schluter. 2008. Adaptation from standing genetic variation. *Trends Ecol. Evol.* 23:38–44.

- Blanchette, M., E. D. Green, W. Miller, and D. Haussler. 2004. Reconstructing large regions of an ancestral mammalian genome in silico. *Genome Res.* 14:2412–2423.
- Bloom, J. D., L. I. Gong, and D. Baltimore. 2010. Permissive secondary mutations enable the evolution of influenza oseltamivir resistance. *Science* 328:1272–1275.
- Blount, Z. D., C. Z. Borland, and R. E. Lenski. 2008. Historical contingency and the evolution of a key innovation in an experimental population of *Escherichia coli*. *Proc. Natl. Acad. Sci. USA* 105:7899–7906.
- Breen, M. S., C. Kemena, P. K. Vlasov, C. Notredame, and F. A. Kondrashov. 2012. Epistasis as the primary factor in molecular evolution. *Nature* 490:535–538.
- Bridgham, J. T., E. A. Ortlund, and J. W. Thornton. 2009. An epistatic ratchet constrains the direction of glucocorticoid receptor evolution. *Nature* 461:515–519.
- Brodie III, E. D., and E. D. Brodie, Jr. 1999. Costs of exploiting poisonous prey: evolutionary trade-offs in a predator-prey arms race. *Evolution* 53:626–631.
- . 2015. Predictably convergent evolution of sodium channels in the arms race between predators and prey. *Brain. Behav. Evol.* 86:48–57.
- . 1990. Tetrodotoxin resistance in garter snakes: an evolutionary response of predators to dangerous prey. *Evolution* 44:651–659.
- Brodie Jr., E. D., B. J. Ridenhour, and E. D. Brodie III. 2002. The evolutionary response of predators to dangerous prey: hotspots and coldspots in the geographic mosaic of coevolution between garter snakes and newts. *Evolution* 56:2067–2082.
- Brown, M. W., F. W. Spiegel, and J. D. Silberman. 2009. Phylogeny of the “forgotten” cellular slime mold, *Fonticula alba*, reveals a key evolutionary branch within Opisthokonta. *Mol. Biol. Evol.* 26:2699–2709.
- Bruen, T. C., H. Philippe, and D. Bryant. 2006. A simple and robust statistical test for detecting the presence of recombination. *Genetics* 172:2665–2681.
- Castoe, T. A., A. P. J. de Koning, H.-M. Kim, W. Gu, B. P. Noonan, G. Naylor, Z. J. Jiang, C. L. Parkinson, and D. D. Pollock. 2009. Evidence for an ancient adaptive episode of convergent molecular evolution. *Proc. Natl. Acad. Sci. USA* 106:8986–8991.
- Castoe, T. A., and C. L. Parkinson. 2006. Bayesian mixed models and the phylogeny of pitvipers (Viperidae: Serpentes). *Mol. Phylogenet. Evol.* 39:91–110.
- Chang, B. S. W., K. Jönsson, M. A. Kazmi, M. J. Donoghue, and T. P. Sakmar. 2002. Recreating a functional ancestral archosaur visual pigment. *Mol. Biol. Evol.* 19:1483–1489.
- Christin, P.-A., D. M. Weinreich, and G. Besnard. 2010. Causes and evolutionary significance of genetic convergence. *Trends Genet.* 26:400–405.
- Clement, M., D. Posada, and K. A. Crandall. 2000. TCS: a computer program to estimate gene genealogies. *Mol. Ecol.* 9:1657–1659.
- Colosimo, P. F., K. E. Hosemann, S. Balabhadra, G. Villarreal Jr., M. Dickson, J. Grimwood, J. Schmutz, R. M. Myers, D. Schluter, and D. M. Kingsley. 2005. Widespread parallel evolution in sticklebacks by repeated fixation of ectodysplasin alleles. *Science* 307:1928–1933.
- Corander, J., P. Marttinen, J. Sirén, and J. Tang. 2008. Enhanced Bayesian modelling in BAPS software for learning genetic structures of populations. *BMC Bioinformatics* 9:539.
- Darriba, D., G. L. Taboada, R. Doallo, and D. Posada. 2012. jModelTest 2: more models, new heuristics and parallel computing. *Nat Meth* 9:772–772.
- DePristo, M. A., D. M. Weinreich, and D. L. Hartl. 2005. Missense mean-derings in sequence space: a biophysical view of protein evolution. *Nat. Rev. Genet.* 6:678–687.
- Dong, K. 2007. Insect sodium channels and insecticide resistance. *Invert. Neurosci.* 7:17.
- Excoffier, L., and H. E. L. Lischer. 2010. Arlequin suite ver 3.5: a new series of programs to perform population genetics analyses under Linux and Windows. *Mol. Ecol. Resour.* 10:564–567.
- Feldman, C. R., E. D. Brodie Jr., E. D. Brodie III, and M. E. Pfrender. 2012. Constraint shapes convergence in tetrodotoxin-resistant sodium channels of snakes. *Proc. Natl. Acad. Sci. USA* 109:4556–4561.
- . 2010. Genetic architecture of a feeding adaptation: garter snake (*Thamnophis*) resistance to tetrodotoxin bearing prey. *Proc. R. Soc. B Biol. Sci.* 277:3317–3325.
- . 2009. The evolutionary origins of beneficial alleles during the repeated adaptation of garter snakes to deadly prey. *Proc. Natl. Acad. Sci. USA* 106:13415–13420.
- Fozzard, H. A., and G. M. Lipkind. 2010. The tetrodotoxin binding site is within the outer vestibule of the sodium channel. *Mar. Drugs* 8:219–234.
- Geffeney, S., E. D. Brodie, Jr., P. C. Ruben, and E. D. Brodie III. 2002. Mechanisms of adaptation in a predator-prey arms race: TTX-resistant sodium channels. *Science* 297:1336–1339.
- Geffeney, S. L., E. Fujimoto, E. D. Brodie III, E. D. Brodie, Jr., and P. C. Ruben. 2005. Evolutionary diversification of TTX-resistant sodium channels in a predator-prey interaction. *Nature* 434:759–763.
- Goldin, A. L. 2002. Evolution of voltage-gated Na⁺ channels. *J. Exp. Biol.* 205:575–584.
- Gompel, N., and B. Prud’homme. 2009. The causes of repeated genetic evolution. *Dev. Biol.* 332:36–47.
- Gong, L. I., M. A. Suchard, and J. D. Bloom. 2013. Stability-mediated epistasis constrains the evolution of an influenza protein. *eLife* 2:e00631.
- Guindon, S., and O. Gascuel. 2003. A simple, fast, and accurate algorithm to estimate large phylogenies by maximum likelihood. *Syst. Biol.* 52:696–704.
- Hanifin, C. T., and W. F. Gilly. 2015. Evolutionary history of a complex adaptation: tetrodotoxin resistance in salamanders. *Evolution* 69:232–244.
- Hanson-Smith, V., B. Kolaczowski, and J. W. Thornton. 2010. Robustness of ancestral sequence reconstruction to phylogenetic uncertainty. *Mol. Biol. Evol.* 27:1988–1999.
- Harms, M. J., and J. W. Thornton. 2013. Evolutionary biochemistry: revealing the historical and physical causes of protein properties. *Nat. Rev. Genet.* 14:559–571.
- . 2014. Historical contingency and its biophysical basis in glucocorticoid receptor evolution. *Nature* 512:203–207.
- Heinemann, S. H., H. Terlau, W. Stühmer, K. Imoto, and S. Numa. 1992. Calcium channel characteristics conferred on the sodium channel by single mutations. *Nature* 356:441–443.
- Hillis, D. M. 1998. Taxonomic sampling, phylogenetic accuracy, and investigator bias. *Syst. Biol.* 47:3–8.
- Holm, S. 1979. A simple sequentially rejective multiple test procedure. *Scand. J. Stat.* 6:65–70.
- Innan, H., and Y. Kim. 2004. Pattern of polymorphism after strong artificial selection in a domestication event. *Proc. Natl. Acad. Sci. USA* 101:10667–10672.
- Jakobsen, I. B., and S. Easteal. 1996. A program for calculating and displaying compatibility matrices as an aid in determining reticulate evolution in molecular sequences. *Comput. Appl. Biosci.* 12:291–295.
- Janzen, F. J., J. G. Krenz, T. S. Haselkorn, E. D. Brodie, Jr., and E. D. Brodie III. 2002. Molecular phylogeography of common garter snakes (*Thamnophis sirtalis*) in western North America: implications for regional historical forces. *Mol. Ecol.* 11:1739–1751.
- Jost, M. C., D. M. Hillis, Y. Lu, J. W. Kyle, H. A. Fozzard, and H. H. Zakon. 2008. Toxin-resistant sodium channels: parallel adaptive

- evolution across a complete gene family. *Mol. Biol. Evol.* 25:1016–1024.
- Keenan, K., P. McGinnity, T. F. Cross, W. W. Crozier, and P. A. Prodöhl. 2013. *diveRsity*: an R package for the estimation and exploration of population genetics parameters and their associated errors. *Methods Ecol. Evol.* 4:782–788.
- Kuchta, S. R., and A.-M. Tan. 2005. Isolation by distance and post-glacial range expansion in the Rough-Skinned Newt, *Taricha granulosa*. *Mol. Ecol.* 14:225–244.
- Lee, C. H., D. K. Jones, C. Ahern, M. F. Sarhan, and P. C. Ruben. 2011. Biophysical costs associated with tetrodotoxin resistance in the sodium channel pore of the garter snake, *Thamnophis sirtalis*. *J. Comp. Physiol. A* 197:33–43.
- Leigh, J. W., and D. Bryant. 2015. *popart*: full-feature software for haplotype network construction. *Methods Ecol. Evol.* 6:1110–1116.
- Li, Y., Z. Liu, P. Shi, and J. Zhang. 2010. The hearing gene *Prestin* unites echolocating bats and whales. *Curr. Biol.* 20:R55–R56.
- Librado, P., and J. Rozas. 2009. *DnaSP v5*: a software for comprehensive analysis of DNA polymorphism data. *Bioinformatics* 25:1451–1452.
- Losos, J. B. 2011. Convergence, adaptation, and constraint. *Evolution* 65:1827–1840.
- Mahoney, M. J. 2004. Molecular systematics and phylogeography of the *Plethodon elongatus* species group: combining phylogenetic and population genetic methods to investigate species history. *Mol. Ecol.* 13:149–166.
- Marshall, D. C., C. Simon, T. R. Buckley, and A. Baker. 2006. Accurate branch length estimation in partitioned Bayesian analyses requires accommodation of among-partition rate variation and attention to branch length priors. *Syst. Biol.* 55:993–1003.
- McGlothlin, J. W., J. P. Chuckalovcak, D. E. Janes, S. V. Edwards, C. R. Feldman, E. D. Brodie, Jr., M. E. Pfrender, and E. D. Brodie III. 2014. Parallel evolution of tetrodotoxin resistance in three voltage-gated sodium channel genes in the garter snake *Thamnophis sirtalis*. *Mol. Biol. Evol.* 31:2836–2846.
- McGlothlin, J. W., M. E. Kobiela, C. R. Feldman, T. A. Castoe, S. L. Geffeney, C. T. Hanifin, G. Toledo, F. J. Vonk, M. K. Richardson, E. D. Brodie, Jr., et al. 2016. Historical contingency in a multigene family facilitates adaptive evolution of toxin resistance. *Curr. Biol.* 26:1616–1621.
- McGuire, J. A., C. C. Witt, D. L. Altshuler, J. V. Remsen, K. Zamudio, and J. Sullivan. 2007. Phylogenetic systematics and biogeography of hummingbirds: Bayesian and Maximum Likelihood analyses of partitioned data and selection of an appropriate partitioning strategy. *Syst. Biol.* 56:837–856.
- Mead, L. S., D. R. Clayton, R. S. Nauman, D. H. Olson, and M. E. Pfrender. 2005. Newly discovered populations of salamanders from Siskiyou County California represent a species distinct from *Plethodon stormi*. *Herpetologica* 61:158–177.
- Miller, S. P., M. Lunzer, and A. M. Dean. 2006. Direct demonstration of an adaptive constraint. *Science* 314:458–461.
- Natarajan, C., F. G. Hoffmann, R. E. Weber, A. Fago, C. C. Witt, and J. F. Storz. 2016. Predictable convergence in hemoglobin function has unpredictable molecular underpinnings. *Science* 354:336–339.
- Natarajan, C., N. Inoguchi, R. E. Weber, A. Fago, H. Moriyama, and J. F. Storz. 2013. Epistasis among adaptive mutations in deer mouse hemoglobin. *Science* 340:1324–1327.
- Natarajan, C., J. Projecto-Garcia, H. Moriyama, R. E. Weber, V. Muñoz-Fuentes, A. J. Green, C. Kopuchian, P. L. Tubaro, L. Alza, M. Bulgarella, et al. 2015. Convergent evolution of hemoglobin function in high-altitude Andean waterfowl involves limited parallelism at the molecular sequence level. *PLOS Genet* 11:e1005681.
- Ono, J., A. C. Gerstein, and S. P. Otto. 2017. Widespread genetic incompatibilities between first-step mutations during parallel adaptation of *Saccharomyces cerevisiae* to a common environment. *PLOS Biol.* 15:e1002591.
- Ortlund, E. A., J. T. Bridgham, M. R. Redinbo, and J. W. Thornton. 2007. Crystal structure of an ancient protein: Evolution by conformational epistasis. *Science* 317:1544–1548.
- Payandeh, J., T. Scheuer, N. Zheng, and W. A. Catterall. 2011. The crystal structure of a voltage-gated sodium channel. *Nature* 475:353–358.
- Poelwijk, F. J., D. J. Kiviet, D. M. Weinreich, and S. J. Tans. 2007. Empirical fitness landscapes reveal accessible evolutionary paths. *Nature* 445:383–386.
- Prezeworski, M., G. Coop, and J. D. Wall. 2005. The signature of positive selection on standing genetic variation. *Evolution* 59:2312–2323.
- R Core Team. 2016. R: a language and environment for statistical computing. R Foundation for Statistical Computing, Vienna, Austria.
- Rambaut, A., M. A. Suchard, D. Xie, and A. J. Drummond. 2014. *Tracer v1.6*. Available from <http://beast.bio.ed.ac.uk/Tracer>.
- Raymond, M., and F. Rousset. 1995. *GENEPOP* (Version 1.2): population genetics software for exact tests and ecumenicism. *J. Hered.* 86:248–249.
- Ridenhour, B. 2004. The coevolutionary process: the effects of population structure on a predator-prey system. Indiana University, Bloomington, IN.
- Ridenhour, B. J., E. D. Brodie III, and E. D. Brodie, Jr. 2004. Resistance of neonates and field-collected garter snakes (*Thamnophis* spp.) to tetrodotoxin. *J. Chem. Ecol.* 30:143–154.
- Ronquist, F., M. Teslenko, P. van der Mark, D. L. Ayres, A. Darling, S. Höhna, B. Larget, L. Liu, M. A. Suchard, and J. P. Huelsenbeck. 2012. *MrBayes 3.2*: efficient Bayesian phylogenetic inference and model choice across a large model space. *Syst. Biol.* 61:539–542.
- Rousset, F. 2008. *genepop'007*: a complete re-implementation of the genepop software for Windows and Linux. *Mol. Ecol. Resour.* 8:103–106.
- Salverda, M. L. M., E. Dellus, F. A. Gorter, A. J. M. Debets, J. van der Oost, R. F. Hoekstra, D. S. Tawfik, and J. A. G. M. de Visser. 2011. Initial mutations direct alternative pathways of protein evolution. *PLOS Genet.* 7:e1001321.
- Schliep, K. P. 2011. *phangorn*: phylogenetic analysis in R. *Bioinformatics* 27:592–593.
- Shah, P., D. M. McCandlish, and J. B. Plotkin. 2015. Contingency and entrenchment in protein evolution under purifying selection. *Proc. Natl. Acad. Sci. USA* 112:E3226–E3235.
- Shi, Y., and S. Yokoyama. 2003. Molecular analysis of the evolutionary significance of ultraviolet vision in vertebrates. *Proc. Natl. Acad. Sci. USA* 100:8308–8313.
- Shimodaira, H., and M. Hasegawa. 1999. Multiple comparisons of log-likelihoods with applications to phylogenetic inference. *Mol. Biol. Evol.* 16:1114–1116.
- Smith, J. M., and N. H. Smith. 2002. Recombination in animal mitochondrial DNA. *Mol. Biol. Evol.* 19:2330–2332.
- Stamatakis, A. 2014. *RAxML Version 8*: a tool for phylogenetic analysis and post-analysis of large phylogenies. *Bioinformatics* 30:1312–1313.
- Stephens, M., N. J. Smith, and P. Donnelly. 2001. A new statistical method for haplotype reconstruction from population data. *Am. J. Hum. Genet.* 68:978–989.
- Stern, D. L., and V. Orgogozo. 2009. Is genetic evolution predictable? *Science* 323:746–751.
- Stoltzfus, A., and L. Y. Yampolsky. 2009. Climbing mount probable: mutation as a cause of nonrandomness in evolution. *J. Hered.* 100:637–647.
- Storz, J. F. 2016. Causes of molecular convergence and parallelism in protein evolution. *Nat. Rev. Genet.* 17:239–250.

- Stöver, B. C., and K. F. Müller. 2010. TreeGraph 2: combining and visualizing evidence from different phylogenetic analyses. *BMC Bioinformatics* 11:7.
- Swenson, N. G., D. J. Howard, A. E. M. E. Hellberg, and E. J. B. Losos. 2005. Clustering of contact zones, hybrid zones, and phylogeographic breaks in North America. *Am. Nat.* 166:581–591.
- Tajima, F. 1983. Evolutionary relationship of DNA sequences in finite populations. *Genetics* 105:437–460.
- . 1989. The effect of change in population size on DNA polymorphism. *Genetics* 123:597–601.
- Templeton, A. R., K. A. Crandall, and C. F. Sing. 1992. A cladistic analysis of phenotypic associations with haplotypes inferred from restriction endonuclease mapping and DNA sequence data. III. Cladogram estimation. *Genetics* 132:619–633.
- Terlau, H., S. H. Heinemann, W. Stühmer, M. Pusch, F. Conti, K. Imoto, and S. Numa. 1991. Mapping the site of block by tetrodotoxin and saxitoxin of sodium channel II. *FEBS Lett.* 293:93–96.
- Tikhonov, D. B., and B. S. Zhorov. 2012. Architecture and pore block of eukaryotic voltage-gated sodium channels in view of NavAb bacterial sodium channel structure. *Mol. Pharmacol.* 82:97–104.
- . 2005. Modeling p-loops domain of sodium channel: homology with potassium channels and interaction with ligands. *Biophys. J.* 88:184–197.
- . 2011. Possible roles of exceptionally conserved residues around the selectivity filters of sodium and calcium channels. *J. Biol. Chem.* 286:2998–3006.
- Tokuriki, N., and D. S. Tawfik. 2009. Stability effects of mutations and protein evolvability. *Curr. Opin. Struct. Biol.* 19:596–604.
- Toledo, G., C. Hanifin, S. Geffeney, and E. D. Brodie III. 2016. Convergent evolution of tetrodotoxin-resistant sodium channels in predators and prey. Pp. 87–113 in R. J. F. and S. Y. Noskov, eds. *Current topics in membranes*. Academic Press, Cambridge, MA.
- Wake, D. B. 1991. Homoplasy: the result of natural selection, or evidence of design limitations? *Am. Nat.* 138:543–567.
- Watterson, G. 1975. On the number of segregating sites in genetical models without recombination. *Theor. Popul. Biol.* 7:256–276.
- Weinreich, D. M., N. F. Delaney, M. A. DePristo, and D. L. Hartl. 2006. Darwinian evolution can follow only very few mutational paths to fitter proteins. *Science* 312:111–114.
- Weinreich, D. M., R. A. Watson, and L. Chao. 2005. Perspective: sign epistasis and genetic constraint on evolutionary trajectories. *Evolution* 59:1165–1174.
- Woods, R., D. Schneider, C. L. Winkworth, M. A. Riley, and R. E. Lenski. 2006. Tests of parallel molecular evolution in a long-term experiment with *Escherichia coli*. *Proc. Natl. Acad. Sci. USA* 103:9107–9112.
- Yampolsky, L. Y., and A. Stoltzfus. 2001. Bias in the introduction of variation as an orienting factor in evolution. *Evol. Dev.* 3:73–83.
- Yang, Z. 2007. PAML 4: phylogenetic analysis by maximum likelihood. *Mol. Biol. Evol.* 24:1586–1591.
- Yokoyama, S., and F. B. Radlwimmer. 2001. The molecular genetics and evolution of red and green color vision in vertebrates. *Genetics* 158:1697–1710.
- Yoon, H.-S., and D. A. Baum. 2004. Transgenic study of parallelism in plant morphological evolution. *Proc. Natl. Acad. Sci. USA* 101:6524–6529.
- Zhang, J., and M. Nei. 1997. Accuracies of ancestral amino acid sequences inferred by the parsimony, likelihood, and distance methods. *J. Mol. Evol.* 44:S139–S146.

Associate Editor: G. Rosenthal

Handling Editor: P. Tiffin

Supporting Information

Additional Supporting Information may be found in the online version of this article at the publisher's website:

Figure S1. Dose-response curves of phenotypic TTX resistance for populations of *T. sirtalis* assayed in this study.

Figure S2. Population estimates of phenotypic TTX resistance for populations assayed for the first time in this study.

Figure S3. Primer sequences.

Figure S4. Nucleotide variation in the full *SCN4A* protein-coding sequence in two focal populations of *T. sirtalis* from the geographically distinct hotspots.

Figure S5. Pairwise F_{ST} estimates for all polymorphic synonymous and nonsynonymous positions in the full *SCN4A* protein-coding sequence.

Figure S6. Phylogenetic and BAPS analyses of the reduced dataset (excluding 1144 bp fragment of exon 26 coding sequence).